



RESEARCH ARTICLE

DEVELOPMENT, SCREENING AND OPTIMIZATION OF ROSUVASTATIN LOADED NANOSTRUCTURED LIPID CARRIERS FOR IMPROVED THERAPEUTIC EFFICACY

El Sayed Gamal E. Shaheen¹, Walid Anwar^{1*}, Sherif K. Abu-Elyazid¹, Mohsen I. Afouna¹

Pharmaceutics Department, Faculty of Pharmacy, Al-Azhar University, Nasr City, Cairo, Egypt.

Article Info:

Abstract



Article History:

Received: 11 July 2024

Reviewed: 15 September 2024

Accepted: 22 October 2024

Published: 15 November 2024

Cite this article:

Shaheen ESGE, Anwar W, Abu-Elyazid SK, Afouna MI. Development, screening and optimization of rosuvastatin loaded nanostructured lipid carriers for improved therapeutic efficacy. Universal Journal of Pharmaceutical Research 2024; 9(5): 82-90.

<http://doi.org/10.22270/ujpr.v9i5.1212>

*Address for Correspondence:

Dr. Walid Anwar, Pharmaceutics Department1, Faculty of Pharmacy, Al-Azhar University, Nasr City, Cairo, Egypt. Tel: +002 010 66429953; E-mail: wawar8182@azhar.edu.eg

Objective: the aim of the current study was to be screening of the formulation components, prepare ROS-NLCs by hot homogenization–ultrasonication technique and optimized by Full factorial design then formulations prepared were further characterized.

Methods: The screening experiments were carried out to select the most suitable solid lipids, liquid lipids, and surfactants. Moreover, physical compatibility between the solid lipids and liquid lipids, along with their proportions, was evaluated. Additionally, characterization and optimization of the developed formulations were outlined and identified. Primarily, the solubility of ROS-Ca in various solid lipids and liquid lipids is the key factor for choosing the optimal one.

Results: Stearic acid, Glyceryl Monostearate (GMS), and Compritol®888 ATO exhibited a higher ability to solubilize ROS-Ca, with solid lipid values per 10 mg of ROS-Ca (w/w) recorded as 750 ± 3.56 mg, 1250 ± 4.36 mg, and 1750 ± 5.16 mg, respectively. In the systematic screening of different liquid lipids, Transcutol® HP (98.41 mg/ml), CapryolTM90 (78.64 mg/ml), and Labrafac MC60 (64.36 mg/ml) demonstrated a good affinity for the drug. The (Stearic acid-Transcutol® HP) mixture showed phase separation with oil droplet residue on filter paper, whereas the (GMS-Transcutol® HP) mixture showed no separation and left no oil droplet residue on filter paper. The optimized NLC formulations composed of glyceryl monostearate GMS (solid lipid) and Transcutol® HP (liquid lipid) as lipid phase, poloxamer 188 and Tween 80 (1:1 ratio) as surfactants.

Conclusions: Study concludes the ability of NLCs to improve the oral bioavailability of poorly water-soluble drugs by enhancing solubilization and dissolution rates in the gastrointestinal tract is well-recognized.

Keywords: Glyceryl monostearate, nanostructured lipid carriers, optimization, rosuvastatin calcium.

INTRODUCTION

Rosuvastatin Ca (ROS-Ca) is a statin drug acting as a competitive inhibitor of HMG-CoA (3-hydroxy-3-methylglutaryl coenzyme A) reductase, which catalyzes the conversion of HMG-CoA to mevalonate, the rate limiting step in cholesterol biosynthesis. Rosuvastatin Ca (ROS-Ca) is a class II drug in Biopharmaceutical Classification System (BCS) which is lipophilic ($\log p \sim 1.92$) in nature and has an oral bioavailability of nearly 20%¹. ROS-Ca has low oral bioavailability which is attributed to its poor aqueous solubility.

To overcome previously mentioned drawbacks and enhance oral bioavailability and aqueous solubility of ROS-Ca, nanostructured lipid carrier (NLCs) second generation of solid lipid nanoparticles (SL) can be

used. In recent decades, lipid-based drug delivery systems have sparked optimism for their positive effects on drug absorption. While conventional lipid-based systems, such as micelles, liposomes, and nano emulsions, have shown promising results, they are vulnerable to degradation during storage and in the gastrointestinal tract (GIT) due to the stomach's acidic environment, intestinal enzymes, and bile salts².

To overcome these limitations, Muller *et al.* extensively researched biocompatible and biodegradable solid lipids, leading to the development of solid lipid nanoparticles (SLNs) in the early 1990s, resolving stability and toxicity concerns associated with conventional lipid-based systems. However, SLNs faced drawbacks like poor drug loading capacity and drug expulsion during storage due to their transformation from a highenergy state to a more

ordered state (β) on storage. To address these issues, modified lipid nanoparticles, also known as nanostructured lipid carriers (NLCs), emerged in the early 2000s to adjust the physical state and drug loading capacity of SLNs³.

NLCs exhibit distinctive characteristics and are formulated using a blend of solid and liquid lipids, generating less ordered structures that enable better inclusion of drug molecules within the matrix during the shelf life⁴. Consistent reports highlight that the increased entrapment efficiency in NLCs is attributed to the structural parity of two lipids in NLCs, resulting in imperfections in their structure, while solidification provides more space for accommodating drugs. Moreover, the higher entrapment efficiency is a result of greater drug solubility in liquid lipids compared to solid lipids⁵. This, along with extended shelf storage stability, positions NLCs as an advanced carrier compared to other traditional lipid-based methods. Furthermore, NLCs have the potential to incorporate both hydrophilic and lipophilic drugs. Additionally, they may facilitate sustained drug release and target drugs to the desired site of action. The system also holds promise for treating chronic diseases due to its modulation of drug efficacy and sustained effects over longer periods. This review primarily delves into the composition and fabrication process of NLCs, examining their properties and their role as a delivery vehicle in enhancing the oral bioavailability of various drugs, along with advancements made to further enhance their performance⁶.

Therefore, the present study was aimed to screen of the formulation components, prepare ROS-NLCs, optimize the preparation and characterization methods of Nanostructured lipid carriers (NLCs) for poorly water-soluble drug (Rosuvastatin Ca, ROS-Ca) to enhance the oral bioavailability⁷.

MATERIALS AND METHODS

The active drug Rosuvastatin calcium (ROS-Ca) was obtained from EIPICO, Cairo –Egypt. Compritol® 888 ATO (glyceryldibehenate), Precirol® ATO 5 (Glycerol distearate type I), Maisine®CC (glyceryl-monolinoleate), LabrafactMPG (propylene glycol dicaprylate/dicaprate), Cprylol® 90 (propylene glycol monocaprylate type II), Labrasol® ALF (caprylo-caproyl macrogol-8-glycerides), Gelucire® 44/14 (lauroyl macrogol-32 glycerides), Gelucire®39/01 pellets (Glycerol esters of saturated C12-C18 fatty acid ester), Transcutol® HP (Highly purified diethylene glycol monoethyl ether) and Labrafil® M2125 CS (linoleoyl macrogol-6-glycerides, were kindly provided as a gift samples from Gattefosse (France). Glyceryl Mono Stearate (GMS), Stearic acid, Poloxamer 188 (polyoxyethylene-polyoxypropylene (150:29) block copolymer), Tween® 80 (polyoxyethylene (20) sorbitanmonooleate), Chitosan, Methanol and Cremophor® EL (polyethoxylated castor oil) were purchased from Sigma Aldrich, Inc. (USA).

Selection of solid lipids

Determination of saturation solubility of ROS-Ca in different solid lipids was performed by the test tube

method. Accurately weighed amount of the ROS-Ca (10 mg) putted in the test tube then the solid lipid was added in increments of (250 mg) which could be heated to 4-5°C above the melting point of the solid lipid with continuous stirring using magnetic stirrer with hot plate at 200 rpm (Remi Instrument Ltd., Mumbai, India).

The quantity of solid lipid required to solubilize ROS-Ca was recorded. The full dissolution state was completed by formation of clear and transparent solution⁸.

Selection of liquid lipids

Screening of liquid lipids was performed by determination of saturation solubility of ROS-Ca in different oils which was performed by adding excess amount of drug in small glass vials contain fixed volume (5 ml) of different liquid lipids. The vials were tightly closed and continuously stirred to reach equilibrium for 72 h at 37°C at 100 rpm using shaker⁹. After that liquid lipids and ROS-Ca mixtures were centrifuged using a high-speed centrifuge (Biofuge Primo centrifuge maximum 17.000 rpm, (England)). at 10,000 rpm for 15 min at 25°C. The supernatant was separated, dissolved in methanol and solubility was quantified by UV-Vis Spectrophotometer (Ultraviolet spectrophotometer, Shimadzu 1800, (Japan)) at 244 nm.

Physical compatibility of solid lipids and liquid lipids

The miscibility of selected solid lipids and liquid lipids that have the maximum affinity for the drug could be achieved. A constant ratio of 1:1 between solid lipids and liquid lipids was used, and the components were melted together in separate glass test tubes. The molten lipid mixture was left to solidify at room temperature. Once solidified, the test tubes were visually examined to confirm the absence of layered separation in the lipid mass. Additionally, the compatibility of the solid and liquid lipids was assessed by applying a cooled sample of the solidified lipid mixture onto a piece of filter paper, followed by a visual check for the presence of oil droplets. A binary mixture with a melting point exceeding 44°C, which showed no oil droplet residues on the filter paper, was selected for the preparation of ROS-NLCs¹⁰⁻¹².

Selection of a binary lipid phase ratios

The ratio of selected solid lipids and liquid lipids was determined based on the melting point of the binary lipid mixture. Selected solid and liquid lipids were blended in the ratio varying from 90:10 to 10:90, then the binary Lipid mixtures were melted and stirred at 200 rpm for 1 h at 5°C above the melting point of solid lipid using hot plate magnetic stirrer. Then, the resulting blend was left to congeal at room temperature. The melting points of the congealed lipid mixtures was determined by capillary method^{13,14}.

Selection of surfactants

For the preparation of NLC, surfactants were selected based on their capacity to emulsify solid liquid binary mixture. Binary lipid mixture (100 mg) was dissolved in 3 ml of methylene chloride and added to 10 ml of 5% surfactant solutions then stirred by magnetic stirrer (Remi Instrument Ltd., Mumbai, India).

The organic layer was evaporated at 40°C and the remaining suspensions were diluted with 10-fold distilled water. The transmittance percent of the resultant samples was determined using UV-Vis spectrophotometer at 510 nm^{9,13}.

Fabrication of nanostructured lipid carriers (NLCs)
Nanostructured lipid carriers containing ROS-Ca (ROS-NLCs) were developed using the hot homogenization-ultrasonication method, incorporating slight modifications. In summary, a predetermined quantity of a binary lipid mixture (solid-to-liquid ratio of 70:30) was melted at a temperature 5 °C above the solid lipid's melting point. ROS-Ca (5% w/w of total lipids) was dissolved in the prepared oil phase, which consisted of 5% w/w of the solid and liquid lipids. The aqueous phase, containing a specific surfactant, was heated to match the oil phase temperature and added gradually (drop wise) under continuous magnetic stirring at 1500 rpm for 10 minutes. Subsequently, the resulting pre-emulsion was homogenized at a high

mixing speed of approximately 20,000 rpm using an Ultra-Turrax T25 homogenizer for 10 minutes. The resulting oil-in-water nanoemulsion was then subjected to probe sonication using an ultrasonic processor (GE130, probe CV18, USA) at 60% amplitude for 10 minutes. Finally, the prepared NLC dispersion was allowed to cool to room temperature.

Experimental design for ROS-Ca optimization

A Full factorial design was employed to study the effect of the independent factors on the dependent responses as shown in Table 1 using Design expert version 13 to predict the optimum NLC formula.

The independent variables were lipid concentration (X1) and surfactant concentration (X2), while the dependent variables were particle size (Y1), polydispersity index (Y2) and % entrapment efficiency (Y3)^{10,15,16} as described in Table 1. Nine formulae of Rosuvastatin were obtained according to the experimental design.

Table 1: Variables in the Full factorial design for the preparation of NLCs.

Variables	Low Level (-1)	Medium level (0)	High level (+1)
Independent variables			
X1 = lipid concentration (% w/v)	2	3	4
X2 = Surfactant concentration (% w/v)	1	1.5	2
Dependent variables			
Y1 = Particle size (nm)	Optimum	-	-
Y2 = Poly dispersity index (PDI)	Minimum		
Y3 = % Entrapment efficiency (% w/w)	Maximum		

Characterization of ROS-NLCs

Particle size (PS), polydispersity index (PDI) and zeta potential (ZP) measurement

The particle size (PS) and polydispersity index (PDI) of NLC were measured by dynamic light scattering using Zetasizer (Zetasizer Nano ZS, Malvern Instruments, UK). This principle depends on measuring the Brownian motion which can detect the PS. The Poly Disparity Index (PDI) was determined as a measure of homogeneity. Small valued of PDI indicate a homogeneous population, while PDI values >0.5 indicates high heterogeneity.

The mean diameter and polydispersity index were measured using a Zetasizer Nano-ZS, equipped with a 10 mW He-Ne laser employing the wavelength of 633 nm and a back-scattering angle of 90° at 25°C. The zeta potential is the electrostatic potential at the boundary between the dispersion medium and the stationary layer of fluid attached to the dispersed particle¹⁷. Zeta potential is an important physical property of particles in suspension, being related with their stability and their surface morphology. Therefore, the measurement of this potential can be useful to characterize the stability of NLCs for an extended period. The zeta potential of NLC formulations was determined via electrophoretic mobility measurements using a (Zetasizer Nano ZS, Malvern Instruments, UK). The zeta potential was calculated by applying the Helmholtz–Smoluchowski equation (n=3)

To determine the particle size, PDI and zeta potential, Before Photon correlation spectroscopic (PCS)

analysis, ROS-NLCs formulations should be diluted with a certain amount of double-distilled water (1: 200) to get appropriate scattering intensity and the samples were analyzed in triplicate¹⁴.

Entrapment efficiency and drug loading

The entrapment efficiency and drug loading of NLC formulations were determined by the following procedure: initially, 2 ml of NLCs formulations were centrifuged at 100,000 rpm for 1 h at 4°C to evaluate the unentrapped ROS-Ca using cooling ultracentrifuge (Beckman Instruments TLX-120 Optima Ultracentrifuge model 19752 Tokyo, (Japan))³.

After centrifugation, the supernatant was separated, filtered using Millipore VR membrane (0.2 µm) and appropriately diluted with methanol and examined by UV-Vis spectrophotometer at 244 nm to determine the unentrapped drug.

In-vitro drug release

The *in-vitro* release tests were performed for pure ROS, and for equivalent weighed amount of the lyophilized powder of the optimized GMS ROS-NLC. A quantity of each preparation containing 2.5 mg of drug was placed in a firmly sealed dialysis bag of a molecular weight cut-off 12-14 kDa. The dialysis bag was immersed in a flask containing 250 ml of Phosphate buffer pH 6.8 with Tween 20 (0.5% w/w) to confirm more sink conditions. The flasks were kept in a shaking water bath (Model 1031; GFL Corporation, Burgwedel, Germany) at 37°C and 100 rpm^{1,8,18}. The parameters of the *in vitro* release study were selected to achieve the sink condition. Aliquots of 2 mL were

withdrawn at time intervals (0.5, 1 h, 2 h, 4 h, 6 h, 8 h, 10 h, 12 h, 18 h and 24 h) with immediate replacement with equal volume of fresh dissolution media to maintain sink conditions. All samples were filtered through 0.250 μm syringe filter¹⁹, The quantity of ROS in the withdrawn samples was determined spectrophotometrically at 244 nm. The experiment was done in triplicate for each formulation and mean values were calculated.

The data are presented as mean \pm SD and were analyzed using one-way ANOVA with GraphPad Prism software version 6.07 (GraphPad, San Diego, California). A p-value of less than 0.05 was considered statistically significant.

RESULTS AND DISCUSSIONS

Selection of solid lipids (SL)

The ability of nanostructured lipid carrier (NLC) formulations to incorporate a specific drug is predominantly influenced by the drug's solubility within the solid lipid core. To optimize the drug loading (DL) and entrapment efficiency (EE) of the formulated NLC, the solubility of ROS-Ca in various solid lipids was assessed. This evaluation facilitated the selection of an appropriate solid lipid for the NLC formulation. A strong affinity between the solid and liquid lipids may ensure high entrapment efficiency, which is a crucial characteristic of a carrier system.

Figure 1 represents the solubility of ROS-Ca in different solid lipids. The experiments with solid lipids demonstrated that the affinity of ROS-Ca to solid lipid was in order of stearic acid < Glyceryl Mono Stearate (GMS) < Compritol®888ATO < Precirol®ATO 5 < Gelucire® 43/01 < Gelucire® 39/01. These results are

in accordance with the work done by authors and scientists.

Stearic acid, Glyceryl Monostearate (GMS) and Compritol®888 ATO showed higher ROS-Ca solubilizing ability, with solid lipid values per 10 mg of ROS-Ca (w/w) of 750 \pm 3.56 mg, 1250 \pm 4.36 mg and 1750 \pm 5.16 mg, respectively. These results correlated with chemical structure of ROS-Ca that contain nitrogen (N) atoms which form hydrogen bonds with stearic acid also due to weak lipophilicity of ROS-Ca (log p ~ 1.9) which allows easier accommodation and higher solubility of the drug in this SL. The high solubility of ROS-Ca in stearic acid and Glyceryl Mono Stearate (GMS) is also due to their self-emulsifying properties^{8,20}.

Selection of liquid lipids (LL)

Adequate dissolvability of ROS-Ca in liquid lipids is fundamental for the effective formulation of nanostructured lipid carriers, as the drug's solubility directly impacts the entrapment efficiency. The screening of liquid lipids was conducted based on the solubility of ROS-Ca in various liquid lipids. The drug-loading capability of the oil phase is a key consideration in their selection for NLC formulation. Higher drug solubility in the oil phase reduces the need for surfactants, thereby minimizing their toxic effects.

The solubility of ROS-Ca in various oils was shown in Figure 2. It was evident that ROS-Ca revealed highest solubility in Transcutol® HP (98.41 mg/ml), Capryol™90 (78.64 mg/ml) and Labrafac MC60 (64.36 mg/ml). The least solubility was observed in Labrasol ALF (39.09 mg/ml), Labrafil M 2125 CS (25.58 mg/ml) and Maisine®CC (16.62 mg/ml). The same results were reported in a previous study²¹.

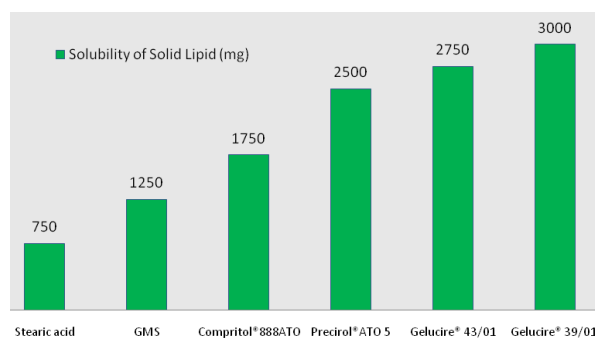


Figure 1: Solubility study of ROS-Ca in different SL.

The solubilization capability of Transcutol® HP (98.41 mg/ml), Capryol™ 90 (78.64 mg/ml), and Labrafac MC60 (64.36 mg/ml) for ROS-Ca is due to their intrinsic self-emulsifying properties and chemical composition (PEG-medium chain triglycerides). PEG/glycerides are believed to possess a superior ability to encapsulate a broad spectrum of lipophilic and hydrophilic drug molecules within lipid carriers, thanks to their well-known surfactant characteristics²².

Physical compatibility of solid lipids and liquid lipids

The miscibility of the chosen solid and liquid lipids with the highest affinity for ROS-Ca was successfully achieved. This step is crucial for ensuring the

development of stable NLCs, as it allows the liquid lipid to be fully incorporated within the solid lipid matrix. To evaluate the physical compatibility of the selected solid lipids (stearic acid, GMS, and Compritol®888 ATO) with the chosen liquid lipid (Transcutol® HP), both visual inspection and filter paper tests were conducted. The above criteria were investigated in previous studies¹⁰⁻¹². (Stearic acid - Transcutol® HP) mixture showed phase separation and residue of oil droplets on filter paper indicating formation of inhomogeneous mixtures. On the other hand, no separation was observed in the congealed mass and no residue of oil droplets on filter paper of (GMS-Transcutol® HP) and (Compritol®888 ATO-

Transcutol® HP) mixtures indicate that formation of homogenous mixture²².

Selection of a binary lipid phase ratios

The ratio of selected solid lipids and liquid lipids was determined based on the melting point of the binary lipid mixture. It was observed that the solid-liquid lipid blends in a 70:30 ratio exhibited an adequate melting point (55–59°C). When the liquid lipid content was increased further, the melting point of the blends fell below the desired level. Therefore, the 70:30 ratio was selected as the standard for the solid-liquid lipid mixture in all NLC formulations. Moreover, the 70:30 ratio is the most suitable and commonly used ratio, as supported by numerous previous studies²³⁻²⁵.

Selection of surfactants

The ability to emulsify and the stability of the emulsion were used as the criteria for selecting surfactants. A higher percentage of transmittance indicates smaller

particle sizes, leading to better emulsification. Additionally, surfactants play a crucial role in stabilizing NLC by decreasing the interfacial tension between the dispersed phase and the dispersion medium, thus preventing particle coalescence and agglomeration. As shown in Table 2 and Table 3, the results demonstrated that Poloxamer 188 (Lutrol® F68, Kolliphor® P 188) exhibited the highest emulsification capacity for the binary lipid mixtures of (Compritrol® 888 ATO - Transcutol® HP) and (GMS - Transcutol® HP), with transmittance values of 93±2% and 90±2%, respectively. This was followed by Tween 80, which had transmittance values of 85±3% and 81±2%, respectively. Finally, Cremophor® EL showed transmittance values of 61±2% and 55±3%, respectively. The percentage of transmittance distinctly reflects the ability of surfactants to emulsify and stabilize selected binary lipid mixtures.

Table 2: Miscibility study of binary lipid mixture with different surfactants.

SAA	GMS and Transcutol® HP Transmittance±SD	Compritrol® ATO 888 and Transcutol® HP
Poloxamer 188	90±2	93±2
Tween 80	81±2	85±3
Cremophore® EL	55±3	61±2

Table 3: Suggested formulae of ROS-NLCs were developed using full factorial design (3²).

Formula	% Lipid Conc.	% SAA Conc.
F1	2	2
F2	2	1.5
F3	3	1.5
F4	4	2
F5	4	1
F6	3	1
F7	4	1.5
F8	2	1
F9	3	2

A high transmittance percentage indicates a well-emulsified and stable emulsion. This is due to the hydrophilic/lipophilic balance (HLB) value of the surfactant used, where higher HLB values are associated with higher transmittance and thus smaller particle sizes. The results obtained align with the work done by previous researchers^{8,20}.

HLB values of surfactants used in screening studies are in order of lutrol®F68 (HLB =29) >Tween® 80(HLB = 15) >Cremophore® EL (HLB = 12-14)²⁶.

Previous studies have shown that using a combination of surfactants is more effective in producing smaller nanoparticles with enhanced storage stability. The results obtained clearly indicated that formulations with more than one surfactant resulted in smaller particle sizes compared to those with a single surfactant. This is due to the combination of multiple surfactants, which create blended surfactant films at the particle level. These blended surfactants efficiently covered the particle surfaces, producing nanoparticles with smaller sizes and providing sufficient viscosity to maintain storage stability. Here, 1:1 ratio of poloxamer 188 and Tween 80 showed excellent emulsification capacity of binary lipids and stability of emulsion ((Compritrol® 888 ATO - Transcutol® HP) and (GMS

- Transcutol® HP), with transmittance values of 96±2% and 93±2%, respectively); hence, poloxamer 188 and Tween 80 in 1:1 ratio was selected as surfactant for the preparation of NLC.

Fabrication and optimization of nanostructured lipid carriers (NLCs)

Based on screening and solubility studies, the NLC formulations were designed, formulated, and optimized. The lipid phase consisted of GMS as solid lipid and Transcutol® HP as the liquid lipid, selected based on the solubility of ROS-Ca in the lipid phase. Poloxamer 188 and Tween 80 mixture (1:1) were chosen as surfactants for the aqueous phase. The ratio of the lipid phase to surfactant was optimized by design expert Full factorial design (3²), and the concentration of ROS-Ca was fixed at 5% (w/w) of the lipid phase. The lipid phase should not exceed 5% (w/w). These observations are consistent with some previous studies by^{22,26}, who found that higher lipid concentrations lead to significantly larger particle sizes. As the formulations were intended for oral use, surfactants were kept at a maximum concentration of 2.5% (w/w). The composition of the formulations is provided in Table 3. Preparation of ROS-NLCs was performed using homogenization followed by the probe sonication

technique. The impact of variations in lipids and surfactants on particle size, PDI and EE was studied. Additionally, other physical characterizations were conducted for each formulation to select the best one for further investigations.

Effects of lipid (X_1) and Surfactant(X_2) concentration on particle size PS (Y_1)

The particle size of ROS-NLC formulations was in the nanometer range. This is shown in Table (5). This reduction significantly impacts the bioavailability of poorly water-soluble compounds. It is well-documented that reducing the particle size to the sub-micron level enhances the dissolution rate and absorption of the compound, thereby improving its bioavailability^{27,28}.

The particle size for better permeation should be less than 500 nm, as represented in Table 4, the observations revealed that all the designed formulations were in the colloidal nanometer range (<300 nm). It can be concluded that particle size of GMS nanoparticles (F1-F9) ranged from (93±1.5 to 270±3 nm).

It was observed that increased lipid concentrations lead to significantly larger particle sizes.

$$PS (Y_1) 190.78 = 17.67(X_1) + 31.67(X_2) - 42.00(X_1X_2) - 39.67(X_1^2) + 31.33(X_2^2)$$

It was shown in the previous equation and Figure 3 that an increase in lipid (X_1) and SAA (X_2) concentrations led to progressive increase in particle size (Y_1).

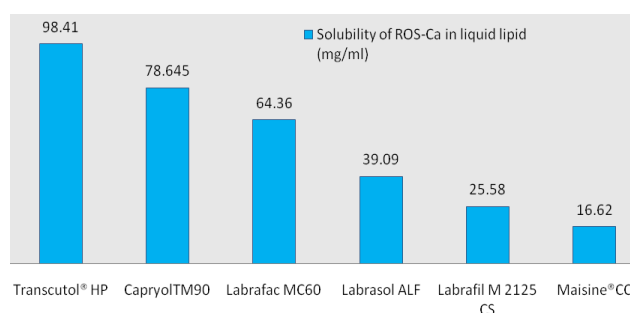


Figure 2: Histogram showing the solubility study of (ROS-Ca) in different LL.

Effects of lipid (X_1) and Surfactant (X_2) concentration on polydispersity index PDI (Y_2)

PDI should be less < 0.5 for better uniformity or mono distribution lower values indicate more homogenous nano dispersions than higher values. Usually, values < 0.5 and considered acceptable concerning the homogeneity of the prepared dispersions²⁹.

Table 5 provides a summary of the polydispersity index measurements. The NLC dispersions produced had a PDI value of $\leq 0.5 \pm 0.02$, owing to the preparation method employed, which indicates a homogeneous and narrow size distribution of NLC nanoparticles^{30,31}.

$$PDI (Y_2) 0.5378 = -0.0150 (X_1) + 0.0033 (X_2) - 0.0650 (X_1X_2) - 0.1317(X_1^2) - 0.0067 (X_2^2)$$

It was shown in the previous equation and Figure 4 that increased lipid concentration decreased the PDI, whereas increased SAA concentration increased the PDI.

Effects of lipid (X_1) and Surfactant (X_2) concentration on Entrapment Efficiency % EE (Y_3)

EE and LC, the amount of drug encapsulated in the nanoparticles and the drug content within the lipid matrix are crucial factors in optimizing NLC. Several factors influence the quantity of drug encapsulated in the lipid matrix, including the type of lipids used, the physicochemical properties of the drug, the drug's miscibility and solubility in the molten lipid, the physical and chemical nature of the lipid matrix, and the crystalline state of the lipid matrix. Additionally, surfactant presence was found to affect encapsulation efficiency. These findings were reported in some previous studies^{8,20}. The entrapment efficiency of all NLCs formulations is presented in Table 5.

It was noted that the EE of ROS-Ca in GMS nanoparticles (F1 to F9) varied from $48 \pm 2\%$ to $73 \pm 2\%$.

$$EE (Y_3) 73.11 = 7.00 (X_1) - 5.00 (X_2) + 3.25 (X_1X_2) - 12.76 (X_1^2) + 2.33(X_2^2)$$

Table 4: Particle size, polydispersity index, zeta potential and entrapment efficiency of ROS-NLCs contain GMS as SL formulations.

F	SL/LL 70: 30 GMS: Trans	SAA 1: 1 T80: P88	PS (nm)±SD	PDI±SD	ZP (mV) ±SD	EE (%)±SD
F1	2	2	270±3	0.48±0.03	-32.9±1.23	48±2
F2	2	1.5	100±1	0.42±0.05	-15.66±1.24	50±3
F3	3	1.5	161±2	0.48±0.03	-27.03±2.13	73±1.5
F4	4	2	173±2	0.29±0.02	-22.13±1.65	65±3
F5	4	1	164±1.7	0.42±0.03	-27.03±2.14	71±2
F6	3	1	235±3.2	0.55±0.04	-34.05±2.65	68±2
F7	4	1.5	232±2.8	0.45±0.03	-23.60±1.87	71±1.4
F8	2	1	93±1.5	0.35±0.02	-21.95±1.68	67±2
F9	3	2	239±3.4	0.57±0.02	-27.26±2.14	73±2

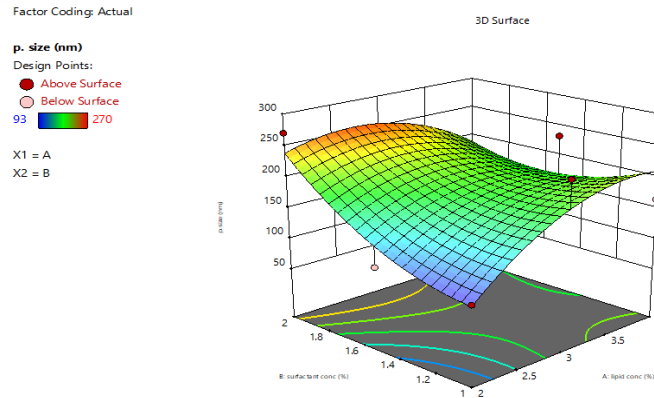


Figure 3:3D plot showing simultaneous influence of independent variables on PS.

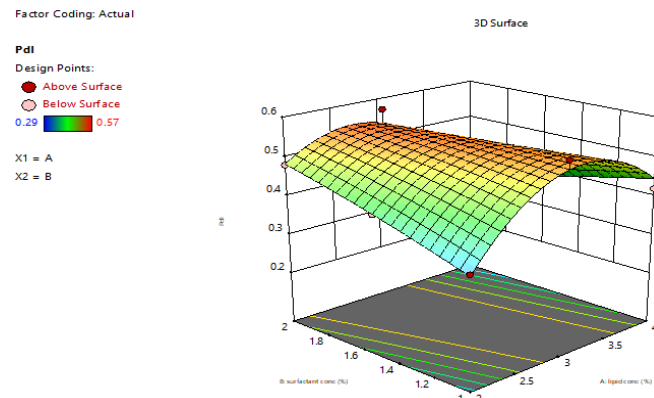


Figure 4: 3D plot showing simultaneous influence of independent variables on PDI.

It was shown in the previous equation and Figure 5 that an increase in lipid concentration resulted in a higher EE% as increased lipid content provides a large space for drug encapsulation, but an increase in SAA concentration caused a decrease in EE%.

Zeta potential (ζ) measurement

Zeta potential provides valuable insights into the surface charge properties and the long-term physical stability of the NLCs. For NLCs stabilized solely by electrostatic repulsion, a minimum zeta potential between -30 and 30 mV is necessary for stability³².

Zeta potential values of all designed formulations are shown in Table 5. The results revealed that the ZP of the various formulations was consistently negative surface charge. ZP values of GMS nanoparticles (F1-F9) in between (-15.66±1.24 to -34.05± 2.65 mV).

Optimized formula OPT-GMS ROS-NLC

After fitting the results of PS, PDI and EE to design expert full factorial design then analysis of the data was done. The optimized formula was obtained that was (lipid concentration: SAA concentration) (2:1) for GMS ROS-NLC¹⁶.

It was observed that the values of particle size, PDI, and zeta potential of the OPT-GMS ROS-NLC were found to be 126.4±2.6 nm, 0.36±0.03 and -9.5±3.7 mV respectively. It was observed that the entrapment efficiency (EE) and loading capacity (LC) of ROS-Ca in OPT-GMS ROS-NLC were 63±2 and 3.15±0.16%. The cumulative drug release percentages for OPT-GMS ROS-NLC formulation and the ROS-Ca suspension are presented in Table 5 and graphically illustrated in Figure 6.

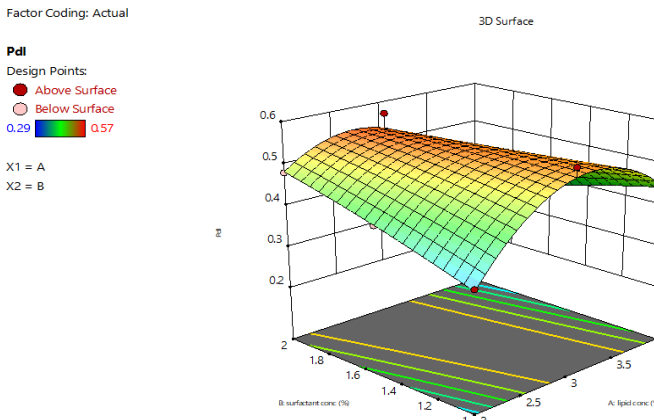


Figure 5: 3D plot showing simultaneous influence of independent variables on EE.

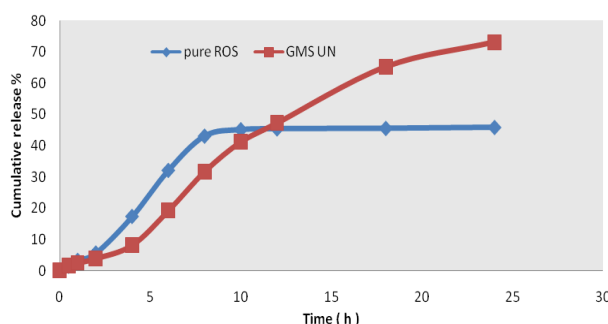


Figure 6: Cumulative release % of ROS from ROS-NLC formulation and ROS Suspension in PBS (pH 6.8).

***In-vitro* release studies of OPT-GMS ROS-NLC**

ROS suspension exhibited a faster drug release in pH 6.8 PBS. Generally, the release of ROS from the suspension was immediate. However, this release process took several hours, suggesting that the dialysis bag provided some resistance approximately 43.12 ± 3.6 % of ROS being released within the first 8 hours. In contrast, ROS was slowly released from GMS ROS-NLC formulation over a period of 24 h approximately 73.16 ± 4.7 % of ROS being released within 24 h.

Additionally, the study found a biphasic release pattern over the 24 h. The initial stage showed a burst effect, typically attributed to the rapid release of the drug embedded on the NLC surface. Following this initial stage, the release of ROS-Ca slowed down. The slow-release phase of ROS-NLCs after the initial stage could be related to the depth of the entrapped ROS in the core matrix of the NLCs³³.

CONCLUSIONS

The ability of NLCs to improve the oral bioavailability of poorly water-soluble drugs by enhancing solubilization and dissolution rates in the gastrointestinal tract is well-recognized. Efficient incorporation of ROS-Ca into NLCs requires careful selection of components and formulation optimization. This study outlines a systematic approach for selecting NLC components through comprehensive screening of excipients to identify the most suitable ones for preparing ROS-NLCs. The formulations developed were subsequently characterized and optimized, resulting in nanoparticles with a favourable size and high entrapment efficiency. In this work, GMS ROS-NLCs were successfully formulated using the hot homogenization-ultrasonication method. The optimized formulations exhibited high entrapment efficiency, significant drug loading, optimal particle size distribution, and an improved dissolution rate by optimizing the lipid-to-surfactant ratios.

ACKNOWLEDGEMENT

The authors extend their thanks and appreciation to the Al-Azhar University, Nasr City, Cairo, Egypt to provide necessary facilities for this work.

AUTHOR'S CONTRIBUTION

Shaheen ESGE: writing original draft, methodology, investigation. **Anwar W:** formal analysis, data curation, conceptualization. **Abu-Elyazid SK:** review and editing. **Afouna MI:** methodology, formal analysis. Final article was checked and approved by all authors.

DATA AVAILABILITY

The accompanying author can provide the empirical data that were utilized to support the study's conclusions upon request.

CONFLICT OF INTEREST

There are no conflicts of interest in regard to this project.

REFERENCES

- Ahmed TA. Development of rosuvastatin flexible lipid-based nanoparticles: Promising nanocarriers for improving intestinal cells cytotoxicity. *BMC Pharmacol Toxicol* 2020; 21:14. <https://doi.org/10.1186/s40360-020-0393-8>
- Javed S, Mangla B, Almoshari Y, Sultan MH, Ahsan W. Nanostructured lipid carrier system: A compendium of their formulation development approaches, optimization strategies by quality by design, and recent applications in drug delivery. *Nanotechnol Rev* 2022; 11:1744-1777. <https://doi.org/10.1515/ntrev-2022-0109>
- Sakellari GI, Zafeiri I, Batchelor H, Spyropoulos F. Formulation design, production and characterisation of solid lipid nanoparticles (SLN) and nanostructured lipid carriers (NLC) for the encapsulation of a model hydrophobic active. *Food Hydrocolloids for Health* 2021; 1:100024. <https://doi.org/10.1016/j.fhfh.2021.100024>
- Nasirizadeh S, Malaekheh-Nikouei B. Solid lipid nanoparticles and nanostructured lipid carriers in oral cancer drug delivery. *J Drug Deliv Sci Technol* 2020; 55:101458. <https://doi.org/10.1016/j.jddst.2019.101458>
- Kim S, Abdella S, Abid F, et al. Development and optimization of imiquimod-loaded nanostructured lipid carriers using a hybrid design of experiments approach. *Int J Nanomed* 2023; 18:1007-1029. <https://doi.org/10.2147/IJN.S400610>
- Khan S, Sharma A, Jain V. An overview of nanostructured lipid carriers and its application in drug delivery through different routes. *Adv Pharm Bull* 2023; 13:446-460. <https://doi.org/10.34172/apb.2023.056>
- Darwish MKM, El-Enin ASMA, Mohammed KHA. Optimized nanoparticles for enhanced oral bioavailability of a poorly soluble drug: Solid lipid nanoparticles versus nanostructured lipid carriers. *Pharm Nanotechnol* 2022;

- 10:69-87.
<https://doi.org/10.2174/2211738510666220210110003>
8. Rizwanullah Md, Amin S, Ahmad J. Improved pharmacokinetics and antihyperlipidemic efficacy of rosuvastatin-loaded nanostructured lipid carriers. *J Drug Target*. 2017; 25:58-74.
<https://doi.org/10.1080/1061186X.2016.1191080>
 9. Dolatabadi S, Karimi M, Nasirizadeh S, et al. Preparation, characterization and *in vivo* pharmacokinetic evaluation of curcuminoids-loaded solid lipid nanoparticles (SLNs) and nanostructured lipid carriers (NLCs). *J Drug Deliv Sci Technol* 2021; 62:102352.
<https://doi.org/10.1016/j.jddst.2021.102352>
 10. Alhalmi A, Amin S, Beg S, Al-Salahi R, Mir SR, Kohli K. Formulation and optimization of naringin loaded nanostructured lipid carriers using Box-Behnken based design: *In vitro* and *ex vivo* evaluation. *J Drug Deliv Sci Technol* 2022; 74:103590.
<https://doi.org/10.1016/j.jddst.2022.103590>
 11. Mathur P, Sharma S, Rawal S, Patel B, Patel MM. Fabrication, optimization, and *in vitro* evaluation of docetaxel-loaded nanostructured lipid carriers for improved anticancer activity. *J Liposome Res* 2020; 30:182-196.
<https://doi.org/10.1080/08982104.2019.1614055>
 12. Sinhmar GK, Shah NN, Chokshi NV, Khatri HN, Patel MM. Process, optimization, and characterization of budesonide-loaded nanostructured lipid carriers for the treatment of inflammatory bowel disease. *Drug Dev Ind Pharm* 2018; 44:1078-1089.
<https://doi.org/10.1080/03639045.2018.1434194>
 13. Date AA, Nagarsenker MS. Single-step and low-energy method to prepare solid lipid nanoparticles and nanostructured lipid carriers using biocompatible solvents. *European J Pharm Res* 2019; 1:12-19.
[https://doi.org/10.34154/2019-EJPR.01\(01\)](https://doi.org/10.34154/2019-EJPR.01(01))
 14. Saghafi Z, Mohammadi M, Mahboobian MM, Derakhshandeh K. Preparation, characterization, and *in vivo* evaluation of perphenazine-loaded nanostructured lipid carriers for oral bioavailability improvement. *Drug Dev Ind Pharm* 2021; 47:509-520.
<https://doi.org/10.1080/03639045.2021.1892745>
 15. Shete MB, Deshpande AS, Shende PK. Nanostructured lipid carrier-loaded metformin hydrochloride: Design, optimization, characterization, assessment of cytotoxicity and ROS evaluation. *Chem Phys Lipids* 2023; 250:105256.
<https://doi.org/10.1016/j.chemphyslip.2022.105256>
 16. Makky AMA, El-leithy SE, Hussein DG, Khattab A. A full factorial design to optimize aminexil nano lipid formulation to improve skin permeation and efficacy against alopecia. *AAPS PharmSciTech* 2023; 24:40.
<https://doi.org/10.1208/s12249-023-02500-3>
 17. Rita Oliveira Macedo Pinto A, Reis S, Nunes C, Lopes D. Amoxicillin-loaded lipid nanoparticles against *Helicobacter pylori* infections 2016.
 18. Li J, Yang M, Xu W. Development of novel rosuvastatin nanostructured lipid carriers for oral delivery in an animal model. *Drug Des Devel Ther* 2018; 12:2241-2248.
<https://doi.org/10.2147/DDDT.S169522>
 19. Parameswaran S, Ramamoorthy VG, Venkateswarlu BS, Chandira RM. Design, 23 factorial optimization and *in vitro-in vivo* pharmacokinetic evaluation of rosuvastatin calcium loaded polymeric nanoparticles. *Int J App Pharm March* 2022;200-205.
<https://doi.org/10.22159/ijap.2022v14i2.43459>
 20. Anwar W, Dawaba HM, Afouna MI, Samy AM. Screening study for formulation variables in preparation and characterization of candesartan cilexetil loaded nanostructured lipid carriers. *Universal J Pharm Res January* 2020. <https://doi.org/10.22270/ujpr.v4i6.330>
 21. Verma R, Kaushik A, Almeer R, et al. Improved pharmacodynamic potential of rosuvastatin by self-nanoemulsifying drug delivery system: An *in vitro* and *in vivo* evaluation. *Int J Nanomedicine* 2021; 16:905-924.
<https://doi.org/10.2147/IJN.S287665>
 22. Nwobodo NN, Adamude FA, Dingwoke EJ, Ubhenin A. Formulation and evaluation of elastic liposomes of decitabine prepared by rotary evaporation method. *Universal J Pharm Res* 2019; 4(3): 1-5.
<https://doi.org/10.22270/ujpr.v4i3.267>
 23. Anwar W, Dawaba HM, Afouna MI, Samy AM, Rashed MH, Abdelaziz AE. Enhancing the oral bioavailability of candesartan cilexetil loaded nanostructured lipid carriers: *In vitro* characterization and absorption in rats after oral administration. *Pharmaceutics* 2020; 12:1-19.
<https://doi.org/10.3390/pharmaceutics12111047>
 24. Yusuf FS, Yunus AA, John DF, Chigbo UJ. Abacavir loaded nanoparticles: preparation, physicochemical characterization and *in vitro* evaluation. *Universal J Pharm Res* 2016; 1(2): 11-14.
<http://doi.org/10.22270/ujpr.v1i2.R2>
 25. Khan I, Hussein S, Houacine C, Khan Sadozai S, Islam Y, Bnyan R, Elhissi A, Yousaf S. Fabrication, characterization and optimization of nanostructured lipid carrier formulations using Beclomethasone dipropionate for pulmonary drug delivery via medical nebulizers. *Int J Pharm* 2021; 598:120376.
<https://doi.org/10.1016/j.ijpharm.2021.120376>
 26. Elbahwy IA, Ibrahim HM, Ismael HR, Kasem AA. Enhancing bioavailability and controlling the release of glibenclamide from optimized solid lipid nanoparticles. *J Drug Deliv Sci Technol* 2017; 38:78-89.
<https://doi.org/10.1016/j.jddst.2017.02.001>
 27. Yuan H, Wang L-L, Du Y-Z, You J, Hu F-Q, Zeng S. Preparation and characteristics of nanostructured lipid carriers for control-releasing progesterone by melt-emulsification. *Colloids Surf B Biointerfaces* 2007; 60:174-179. <https://doi.org/10.1016/j.colsurfb.2007.06.011>
 28. Chaudhari VS, Murty US, Banerjee S. Nanostructured lipid carriers as a strategy for encapsulation of active plant constituents: Formulation and *in vitro* physicochemical characterizations. *Chem Phys Lipids* 2021; 235:105037.
<https://doi.org/10.1016/j.chemphyslip.2020.105037>
 29. Hassan DH, Shohdy JN, El-Setouhy DA, El-Nabarawi M, Naguib MJ. Compritol- based Nanostructured Lipid Carriers (NLCs) for augmentation of zolmitriptan bioavailability via the transdermal route: *In vitro* optimization, *ex vivo* permeation, *in vivo* pharmacokinetic study. *Pharmaceutics*. 2022; 14:1484.
<https://doi.org/10.3390/pharmaceutics14071484>
 30. Das S, Ng WK, Tan RBH. Are nanostructured lipid carriers (NLCs) better than solid lipid nanoparticles (SLNs): Development, characterizations and comparative evaluations of clotrimazole-loaded SLNs and NLCs? *European J Pharm Sci* 2012; 47:139-151.
<https://doi.org/10.1016/j.ejps.2012.05.010>
 31. Izham MNM, Hussin Y, Rahim NFC, et al. Physicochemical characterization, cytotoxic effect and toxicity evaluation of nanostructured lipid carrier loaded with eucalyptol. *BMC Complement Med Ther* 2021; 21:254. <https://doi.org/10.1186/s12906-021-03422-y>
 32. Zafar A, Alruwaili NK, Imam SS, et al. Formulation of chitosan-coated piperine nlc: optimization, *in vitro* characterization, and *in vivo* preclinical assessment. *AAPS PharmSci Tech* 2021; 22.
<https://doi.org/10.1208/s12249-021-02098-4>
 33. Xun M, Guo H, Cui Q, et al. Process validation and *in vitro - in vivo* evaluation of rosuvastatin calcium tablets. *Drug Dev Ind Pharm*. 2022; 48:140-145.
<https://doi.org/10.1080/03639045.2022.2101061>